Stability of core-annular flow with a small viscosity ratio

Howard H. Hu, Thomas S. Lundgren, and Daniel D. Joseph
Department of Aerospace Engineering and Mechanics, University of Minnesota, Minneapolis, Minnesota 55455

(Received 15 March 1990; accepted 24 July 1990)

It is known that the stability problem for core-annular flow of very viscous crude oil and water is singular, the water annulus appears to be inviscid with boundary layers at the pipe wall and at the interface. In the present paper, this singular problem is treated by the method of matched asymptotic expansions using $\epsilon = m/R\alpha$ as a small parameter. There are two cases of instability corresponding to different positions of the critical point in the annulus. One case is when the critical point is far away from the interface, the other is when the critical point is close to the interface within a distance of order $\epsilon^{1/3}$. In both cases, the equations for the eigenvalues are derived, and the explicit forms for the neutral curves are given. The stability problem is also treated by the modified finite element code used by Hu and Joseph [J. Fluid Mech. **205**, 359 (1989); Phys. Fluids A **1**, 1659 (1989)], taking into account the boundary layers at the pipe wall and at the interface. The results of the two methods agree where they overlap, but the finite element technique goes further.

I. INTRODUCTION

There is a strong tendency for two fluids to arrange themselves so that the low-viscosity constituent is in the region of high shear.[1] This gives rise to a kind of gift of nature in which the lubricated flows are stable, and it opens up very interesting possibilities for technological applications in which one fluid is used to lubricate another.

One possible application is lubricated pipelining, the transportation of very viscous crude oils along with an immiscible lubricating liquid, usually water. Experiments to examine this possibility have been carried out by Russell and Charles,[2] Russell, Hodgson, and Govier,[3] Charles, Govier, and Hodgson,[4] Charles and Lilleleht,[5] and Bai, Chen, and Joseph.[6]

Various arrangements of oil and water occur in the aforementioned experiments. This type of nonuniqueness is typical of flowing bicomponent fluids. The arrangements that appear in horizontal pipes are (a) stratified flow with heavy fluid below; (b) concentric oil in water (core-annular flow); (c) water drops in oil; (d) oil drops (bubbles) in water (these include large bubbles and slugs of oil lubricated by water).

The first theoretical stability study of core-annular flow when the core is more viscous was given by Joseph, Renardy, and Renardy.[7] They neglected density differences and surface tension and found that lubricated transport was stable if the water fraction was not too great. This was followed by a numerical study of Preziosi, Chen, and Joseph[8] in which all effects except gravity were considered using a pseudospectral method. They compared their analysis with the experiments of Charles, Govier, and Hodgson,[4] and found many points of agreement between theory and experiment. Hu and Joseph[9] studied the situation when the pipe wall is hydrophobic. They developed an efficient finite element code that worked well even when the ratio of viscosities of water to oil is small. They also computed various terms that arise in the global balance of energy of a small disturbance, which allowed them to identify different sources of instability.

There are significant reserves of heavy viscous crude oils in the world, with viscosity as high as 1000 P at room temperature. Thus in actual applications, the ratio of viscosities of water to oil is usually extremely small, say 10^{-5}. All the studies mentioned above were for larger ratios. For very small ratios the stability problem is singular, the water annulus is nearly inviscid with boundary layers at the pipe wall and at the interface. In this situation direct numerical methods, for example pseudospectral method, do not give reliable results unless special attention is paid to these boundary layers. In the present paper we treat this singular problem by the method of matched asymptotic expansions and by the modified finite element code used by Hu and Joseph,[9,10] taking into account of the boundary layers at the pipe wall and at the interface between the water and oil.

II. FORMULATION OF THE PROBLEM

Two liquids are flowing down a circular pipe of inner radius R_2. The core is occupied by liquid 1 and the annulus by liquid 2. The interface between liquids is $r = R(\theta,x,t)$, where (r,θ,x) are cylindrical coordinates and t is time. Let $\mathbf{U} = (u_r,u_\theta,u_x)$ be velocity, $\hat{p}$ be pressure, μ_1 and μ_2 be viscosities of liquid 1 and liquid 2, and the densities of two liquids are the same $\rho_1 = \rho_2 = \rho$.

The basic flow is a steady, fully developed core-annular flow driven by a constant pressure gradient. The location of the interface for this basic flow is at $r = R_1$, a constant. The velocity profile is parabolic in both core and annulus with a jump in slope at the interface due to the discontinuity of the viscosities of two liquids.

We scale length with the interface radius R_1, velocity with the centerline velocity of the basic flow W_0, pressure with ρW_0^2 and time with R_1/W_0. This leads to the following dimensionless parameters:

$a = R_2/R_1$, the radius ratio,

 0899-8213/90/111945-10$02.00

$m = \mu_2/\mu_1$, the viscosity ratio,

$\mathbb{R} = \rho W_0 R_1/\mu_1$, the Reynolds number based on the core liquid,

$\hat{J} = T\rho R_1/\mu_2^2$, the interfacial tension parameter based on liquid 2, where T is the coefficient of interfacial tension between two liquids.

The form of the basic flow is

$$\mathbf{U} = [0,0,W(r)], \tag{1}$$

where

$$W(r) = \begin{cases} 1 - mr^2/(a^2+m-1), & 0 \leqslant r \leqslant 1, \\ (a^2-r^2)/(a^2+m-1), & 1 \leqslant r \leqslant a. \end{cases} \tag{2}$$

We assume that the disturbances (u,v,w) of velocities, p of pressure, and δ of the interface radius are axisymmetric and proportional to $\exp[i\alpha(x-ct)]$, where α is the dimensionless wave number, $\mathrm{Re}\{c(\alpha)\}$ is the dimensionless velocity of the disturbance of wave number α in the x direction, and $\mathrm{Im}\{\alpha c\}$ is the growth rate of the same disturbances. In our previous works we verified that axisymmetric disturbances are most dangerous.

After eliminating the axial velocity disturbance w and pressure p, the linearized equation for velocity disturbance in the r direction is

$$\frac{1}{\mathbb{R}\alpha}\left(D^2+\frac{1}{r}D-\frac{1}{r^2}-\alpha^2\right)^2 u_1 - i(W-c) \times\left(D^2+\frac{1}{r}D-\frac{1}{r^2}-\alpha^2\right)u_1 = 0, \quad \text{for } 0 \leqslant r \leqslant 1, \tag{3}$$

$$\frac{m}{\mathbb{R}\alpha}\left(D^2+\frac{1}{r}D-\frac{1}{r^2}-\alpha^2\right)^2 u_2 - i(W-c) \times\left(D^2+\frac{1}{r}D-\frac{1}{r^2}-\alpha^2\right)u_2 = 0, \quad \text{for } 1 \leqslant r \leqslant a, \tag{4}$$

where $D = d/dr$. The boundary and interfacial conditions are

$$u_2 = Du_2 = 0, \text{ at the pipe wall } r = a, \tag{5}$$

$$u_1, Du_1, D^2u_1 \text{ are bounded at the origin } r = 0, \tag{6}$$

and at the interface $r = 1$,

$$u_1 = u_2, \tag{7}$$

$$\frac{2(1-m)}{a^2-1+m}u_1 - \left(\frac{a^2-1}{a^2-1+m}-c\right)(Du_1 - Du_2) = 0, \tag{8}$$

$$(D^2+D-1+\alpha^2)u_1 - m(D^2+D-1+\alpha^2)u_2 = 0, \tag{9}$$

$$[D^3+2D^2-(3\alpha^2+1)D+(1-\alpha^2)]u_1 - m[D^3+2D^2-(3\alpha^2+1)D+(1-\alpha^2)]u_2 = im^2\frac{\hat{J}}{\mathbb{R}}\frac{\alpha(1-\alpha^2)}{(a^2-1)/(a^2-1+m)-c}u_1. \tag{10}$$

For further details of these equations, see Preziosi, Chen, and Joseph.[8]

Therefore the problem is to solve the eigensystem of ordinary differential equations (3) and (4) subject to the conditions (5)–(10), when viscosity ratio $m \to 0$, say, very viscous crude oil core being lubricated by water. After examining Eq. (4) we choose

$$\epsilon = m/\mathbb{R}\alpha \tag{11}$$

as a small parameter, and use a matched asymptotic perturbation scheme to solve the problem.

As m or $\epsilon \to 0$, Eq. (3) is regular, and we can get a uniformly valid asymptotic expansion for u_1 in the core region. On the other hand, Eq. (4) is singular, since ϵ is the coefficient for the term that has the highest derivative. We therefore argue that within most of the annulus the viscous force corresponding to the first term is much less important than the inertial force corresponding to the second term and may be neglected. In some regions, however, the viscous force may be of the same order of magnitude as the inertial force. These regions are the viscous boundary layer at the pipe wall where the no-slip boundary condition is required, the viscous boundary layer at the interface where the interfacial conditions are prescribed, and the critical layer where the velocity of the disturbance is the same as the velocity $W(r_c)$ of the basic flow, $\mathrm{Re}\{c\} = W(r_c)$. The asymptotic expansions are different depending on the location of the critical point $r = r_c$. We treat two cases: (a) the critical point is far away from the interface; and (b) the critical point is close to the interface, within a distance of order $\epsilon^{1/3}$, as indicated in Fig. 1. This method of analysis is a standard procedure, and is employed in studying the large $\alpha\mathbb{R}$ limit for unidirectional shear flows with boundaries (e.g., plane Poiseuille flow of a single fluid), see Drazin and Reid.[11]

III. CASE I: THE CRITICAL POINT IS FAR AWAY FROM THE INTERFACE

In this situation, an appropriate expansion for the eigenvalue c is

$$c \sim \sum_{n=0}^{\infty} (\epsilon^{1/2})^n c_n.$$

In the present study, only two terms of the expansion are computed, that is,

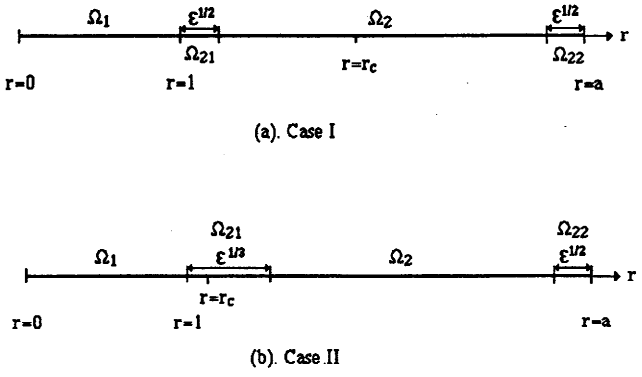

FIG. 1. Two cases considered. (a) The critical point $r = r_c$ is far away from the interface. (b) The critical point is close to the interface, within a distance of order $\epsilon^{1/3}$.

$$c \sim c_0 + \epsilon^{1/2} c_1 + O(\epsilon). \tag{12}$$

The basic flow (2) can be expanded in terms of ϵ as

$$W(r) = \begin{cases} 1 + O(\epsilon), & 0 \leqslant r \leqslant 1, \\ (a^2 - r^2)/(a^2 - 1) + O(\epsilon), & 1 \leqslant r \leqslant a. \end{cases} \tag{13}$$

A. In the core Ω_1

In the core Ω_1 as indicated in Fig. 1(a), the velocity u_1 is expanded as

$$u_1(r) = u_1^{(0)}(r) + \epsilon^{1/2} u_1^{(1)}(r) + O(\epsilon). \tag{14}$$

After substituting (12), (13), and (14) into Eq. (3), and collecting the coefficients for ϵ^0 and $\epsilon^{1/2}$ terms in the equation, we have two equations for $u_1^{(0)}(r)$ and $u_1^{(1)}(r)$:

$$\left(D^2 + \frac{1}{r} D - \frac{1}{r^2} - \kappa^2\right)\left(D^2 + \frac{1}{r} D - \frac{1}{r^2} - \alpha^2\right) u_1^{(0)} = 0, \tag{15}$$

$$\left(D^2 + \frac{1}{r} D - \frac{1}{r^2} - \kappa^2\right)\left(D^2 + \frac{1}{r} D - \frac{1}{r^2} - \alpha^2\right) u_1^{(1)} = -i\mathrm{R}\alpha c_1 \left(D^2 + \frac{1}{r} D - \frac{1}{r^2} - \alpha^2\right) u_1^{(0)}, \tag{16}$$

where

$$\kappa^2 = \alpha^2 + i\mathrm{R}\alpha(1 - c_0). \tag{17}$$

Since the critical point is away from the interface, or $c_0 \neq 1$, we have $\kappa^2 \neq \alpha^2$.

The solutions to Eqs. (15) and (16) with the conditions that the solutions are bounded at the origin are

$$u_1^{(0)}(r) = A_{11} I_1(\kappa r) + A_{12} I_1(\alpha r), \tag{18}$$

$$u_1^{(1)}(r) = -(i\mathrm{R}\alpha c_1/2\kappa) A_{11} r I_0(\kappa r) + B_{11} I_1(\kappa r) + B_{12} I_1(\alpha r), \tag{19}$$

where $I_1(\cdot)$ and $I_0(\cdot)$ are the modified Bessel function of the first kind with order 1 and 0, respectively, A_{11}, A_{12}, B_{11}, and B_{12} are arbitrary constants to be determined by the interfacial conditions later. It is interesting to see that here as $m \to 0$, the basic flow in the core becomes uniform, and Eqs. (15) and (16) can be easily integrated in terms of the Bessel functions rather than the more difficult Kummer functions that are used by Papageorgiou, Maldarelli, and Rumschitzki[12] in integrating the core equation for general m.

B. The form of the solution in the annulus Ω_2

The outer expansion for velocity u_2 in Ω_2 is

$$u_2(r) = u_2^{(0)}(r) + \epsilon^{1/2} u_2^{(1)}(r) + O(\epsilon), \quad \text{in } \Omega_2. \tag{20}$$

After substituting the expansion into Eq. (4), we find that $u_2^{(0)}(r)$ and $u_2^{(1)}(r)$ satisfy

$$\left(D^2 + \frac{1}{r} D - \frac{1}{r^2} - \alpha^2\right) u_2^{(j)} = 0, \quad j = 0,1. \tag{21}$$

Thus the solutions are

$$u_2^{(0)}(r) = A_{21} I_1(\alpha r) + A_{22} K_1(\alpha r), \tag{22}$$

$$u_2^{(1)}(r) = B_{21} I_1(\alpha r) + B_{22} K_1(\alpha r), \tag{23}$$

where $K_1(\cdot)$ is the modified Bessel function of the second kind with order 1, and the A's and B's are arbitrary constants.

We noticed that the solution to the outer Orr–Sommerfeld equation (4) is not singular at the critical point $r = r_c$ for this case since $r(W'/r)'$ is zero (compares to the Eq. 31.16 of Drazin and Reid[11]), thus the outer expansion (20) is smooth at r_c, and there is no need for a critical layer in this case as indicated in Fig. 1(a).

C. The form of the solution in the boundary layer at the pipe wall Ω_{22}

It can be easily verified that the proper choice of scaling for this wall boundary layer Ω_{22} is $\epsilon^{1/2}$, the inner coordinate in the boundary layer is therefore introduced as

$$\eta = (a - r)/\epsilon^{1/2}. \tag{24}$$

The inner expansion for the velocity in this layer takes the form

$$u_2(r) = \epsilon^{1/2} u_{22}^{(0)}(\eta) + \epsilon u_{22}^{(1)}(\eta) + O(\epsilon^{3/2}). \tag{25}$$

Here since the basic flow is of order $\epsilon^{1/2}$ in this layer, the order of the leading term in expansion (25) is taken to be $\epsilon^{1/2}$ too.

By changing to the new variable in Eq. (4), and using the expansion (25), we obtain two equations for $u_{22}^{(0)}$ and $u_{22}^{(1)}$,

$$D_\eta^4 u_{22}^{(0)} + i c_0 D_\eta^2 u_{22}^{(0)} = 0, \tag{26}$$

$$D_\eta^4 u_{22}^{(1)} + i c_0 D_\eta^2 u_{22}^{(1)} = \frac{2}{a} D_\eta^3 u_{22}^{(0)} + i\left[\frac{c_0}{a} D_\eta u_{22}^{(0)} + \left(\frac{2a}{a^2 - 1}\eta - c_1\right) D_\eta^2 u_{22}^{(0)}\right], \tag{27}$$

where D_η stands for $d/d\eta$. The boundary condition (6) transforms to

$$u_{22}^{(0)}(0) = D_\eta u_{22}^{(0)}(0) = u_{22}^{(1)}(0) = D_\eta u_{22}^{(1)}(0) = 0. \tag{28}$$

As $\eta \to \infty$, $u_{22}^{(0)}(\eta)$, $u_{22}^{(1)}(\eta)$ are required to match the outer expansion (20) as $r \to a$.

The solution to (26) satisfying (28) and the matching requirements is

$$u_{22}^{(0)}(\eta) = A_3^{(2)}(e^{p\eta} - p\eta - 1), \tag{29}$$

where $A_3^{(2)}$ is a constant to be determined by the matching, and $p = \pm\sqrt{-ic_0}$ with a negative real part.

Similarly, after substituting (29) into (27) we find the solution

$$u_{22}^{(1)}(\eta) = B_3^{(2)}(e^{p\eta} - p\eta - 1) + iA_3^{(2)}\left[\frac{c_0 \eta^2}{2ap} - \left(\frac{c_0}{a} + c_1 p\right)\frac{1}{2p^2}\left(\eta(e^{p\eta} + 1) - \frac{2}{p}(e^{p\eta} - 1)\right) + \frac{a}{2p(a^2 - 1)} \times \left(\eta^2 e^{p\eta} - \frac{\eta}{p}(5e^{p\eta} + 3) + \frac{8}{p^2}(e^{p\eta} - 1)\right)\right], \tag{30}$$

where $B_3^{(2)}$ is another constant to be determined by matching with the outer solution.

The constants $A_3^{(2)}$ and $B_3^{(2)}$ are determined by match-

ing the inner expansion (25) with the outer expansion (20), which can be done either by introducing an intermediate layer where both expansions are valid as used in Kevorkian and Cole,[13] or simply by a Van Dyke procedure.[14] Note that since the outer expansion (20) is a continuous function at $r=a$, we can represent it by a Taylor series around $r=a$. The matching gives the following relations:

$$u_2^{(0)}(a)=0, \tag{31}$$

$$Du_2^{(0)}(a)=A_3^{(2)}p, \tag{32}$$

$$u_2^{(1)}(a)=-A_3^{(2)}, \tag{33}$$

$$Du_2^{(1)}(a)=B_3^{(2)}p+\frac{iA_3^{(2)}}{2p^2}\left(\frac{c_0}{a}+c_1p+\frac{3a}{a^2-1}\right). \tag{34}$$

In (32) and (33) $A_3^{(2)}$ can be eliminated giving

$$Du_2^{(0)}(a)=-u_2^{(1)}(a)p. \tag{35}$$

D. The form of the solution in the boundary layer at the interface Ω_{21}

Following the procedure used in Sec. III C, an inner coordinate is defined:

$$\xi=(r-1)/\epsilon^{1/2}. \tag{36}$$

The inner expansion for the velocity u_2 takes the form

$$u_2(r)=u_{21}^{(0)}(\xi)+\epsilon^{1/2}u_{21}^{(1)}(\xi)+\epsilon u_{21}^{(2)}(\xi)+O(\epsilon^{3/2}). \tag{37}$$

Here we find it necessary to carry out the expansion to the third term.

At the leading order ϵ^0,

$$D_\xi^4u_{21}^{(0)}-i(1-c_0)D_\xi^2u_{21}^{(0)}=0, \tag{38}$$

with boundary conditions at $\xi=0$ [derived from the interfacial condition (7)–(10)]:

$$\begin{aligned}&u_{21}^{(0)}(0)=u_1^{(0)}(1),\\&D_\xi u_{21}^{(0)}(0)=0,\\&D_\xi^2u_{21}^{(0)}(0)=(1/\mathrm{R}\alpha)(D^2+D-1+\alpha^2)u_1^{(0)}(1),\\&D_\xi^3u_{21}^{(0)}(0)=0.\end{aligned} \tag{39}$$

The solution to this order is a constant

$$u_{21}^{(0)}(\xi)=A_1^{(1)}=u_1^{(0)}(1). \tag{40}$$

The third boundary condition in (39) requires

$$(D^2+D-1+\alpha^2)u_1^{(0)}(1)=0. \tag{41}$$

At the next order $\epsilon^{1/2}$ we have

$$\begin{aligned}D_\xi^4u_{21}^{(1)}-i(1-c_0)D_\xi^2u_{21}^{(1)}&=-2D_\xi^3u_{21}^{(0)}+i\{(1-c_0)D_\xi u_{21}^{(0)}\\&\quad-[2\xi/(a^2-1)+c_1]D_\xi^2u_{21}^{(0)}\}.\end{aligned} \tag{42}$$

The right-hand side of the equation is zero after substituting $u_{21}^{(0)}$ into the equation. The boundary conditions at $\xi=0$ are

$$u_{21}^{(1)}(0)=u_1^{(1)}(1),$$

$$D_\xi u_{21}^{(1)}(0)=Du_1^{(0)}(1)-\frac{2}{a^2-1}\frac{1}{1-c_0}u_1^{(0)}(1),$$

$$D_\xi^2u_{21}^{(1)}(0)=(1/\mathrm{R}\alpha)(D^2+D-1+\alpha^2)u_1^{(1)}(1),$$

$$D_\xi^3u_{21}^{(1)}(0)=(1/\mathrm{R}\alpha)[D^3+2D^2-(3\alpha^2+1)D+1-\alpha^2]u_1^{(0)}(1). \tag{43}$$

The solution is

$$u_{21}^{(1)}(\xi)=B_1^{(1)}+B_2^{(1)}\xi+B_3^{(1)}e^{q\xi}, \tag{44}$$

where $q=\pm\sqrt{i(1-c_0)}$ has a negative real part and the constants satisfy

$$B_1^{(1)}+B_3^{(1)}=u_1^{(1)}(1), \tag{45}$$

$$B_2^{(1)}+qB_3^{(1)}=Du_1^{(0)}(1)-\frac{2}{a^2-1}\frac{1}{1-c_0}u_1^{(0)}(1), \tag{46}$$

$$\mathrm{R}\alpha q^2B_3^{(1)}=(D^2+D-1+\alpha^2)u_1^{(1)}(1), \tag{47}$$

$$\mathrm{R}\alpha q^3B_3^{(1)}=[D^3+2D^2-(3\alpha^2+1)D+1-\alpha^2]u_1^{(0)}(1). \tag{48}$$

A similar derivation was carried out to order ϵ^1. The equation and boundary conditions are lengthy, so only the final result is presented here. We found that

$$\begin{aligned}u_{21}^{(2)}(\xi)&=D_1^{(1)}+D_2^{(1)}\xi+D_3^{(1)}e^{q\xi}-\frac{i(1-c_0)}{2q^2}\\&\quad\times[B_2^{(1)}-(1+\alpha^2)A_1^{(1)}]\xi^2-iB_3^{(1)}\\&\quad\times\frac{1-c_0+c_1q}{2q^2}\left(\xi-\frac{2}{q}\right)e^{q\xi}-iB_3^{(1)}\\&\quad\times\frac{1}{2q(a^2-1)}\left(\xi^2-5\frac{\xi}{q}+\frac{8}{q^2}\right)e^{q\xi},\end{aligned} \tag{49}$$

where $D_1^{(1)}$, $D_2^{(1)}$, and $D_3^{(1)}$ are constants, and $D_2^{(1)}$ can be determined by boundary conditions as

$$\begin{aligned}D_2^{(1)}&=B_3^{(1)}\left(1-\frac{c_1}{1-c_0}q+\frac{2}{(a^2-1)(1-c_0)}\right)-\frac{1}{\mathrm{R}\alpha q^2}\\&\quad\times[D^3+2D^2-(3\alpha^2+1+\mathrm{R}\alpha q^2)D+1-\alpha^2]\\&\quad\times u_1^{(1)}(1)-\frac{2}{(a^2-1)(1-c_0)}\\&\quad\times\left(u_1^{(1)}(1)+\frac{c_1}{1-c_0}u_1^{(0)}(1)\right).\end{aligned} \tag{50}$$

Again the matching with the outer expansion (20) as $r\to1$ gives the relations:

$$u_2^{(0)}(1)=A_1^{(1)}=u_1^{(0)}(1), \tag{51}$$

$$Du_2^{(0)}(1)=B_2^{(1)}, \tag{52}$$

$$u_2^{(1)}(1)=B_1^{(1)}, \tag{53}$$

$$Du_2^{(1)}(1)=D_2^{(1)}. \tag{54}$$

E. The secular equations

At the zeroth order, we group four equations, Eqs. (31), (41), (51), and (46), with $B_3^{(1)}$ and $B_2^{(1)}$ eliminated with (48) and (52), and write them explicitly using the properties of the Bessel functions

$$\begin{aligned}&A_{21}I_1(\alpha a)+A_{22}K_1(\alpha a)=0,\\&(\kappa^2+\alpha^2)A_{11}I_1(\kappa)+2\alpha^2A_{12}I_1(\alpha)=0,\\&A_{21}I_1(\alpha)+A_{22}K_1(\alpha)=A_{11}I_1(\kappa)+A_{12}I_1(\alpha),\end{aligned}$$

$$\alpha[A_{21}I_1'(\alpha)+A_{22}K_1'(\alpha)]-(1/\mathbb{R}\alpha q^2)\{A_{11}[(3\alpha^2-\kappa^2)\times\kappa I_1'(\kappa)-(\kappa^2-\alpha^2)I_1(\kappa)]+A_{12}[2\alpha^3 I_1'(\alpha)]\}$$
$$=[\kappa A_{11}I_1'(\kappa)+\alpha A_{12}I_1'(\alpha)]-\frac{2}{(a^2-1)(1-c_0)}\times[A_{11}I_1(\kappa)+A_{12}I_1(\alpha)].$$

Nonzero solutions A_{11}, A_{12}, A_{21}, and A_{22} of this set of linear equations can be obtained only if the secular equation formed from the determinant of the coefficients is satisfied. This gives

$$4\alpha^4\kappa\frac{I_1'(\kappa)}{I_1(\kappa)}-(\kappa^2+\alpha^2)^2\alpha\frac{I_1'(\alpha)}{I_1(\alpha)}+(\kappa^2-\alpha^2)^2\times\alpha Z+(\kappa^2-\alpha^2)\left(-2\alpha^2+\frac{i2\mathbb{R}\alpha}{a^2-1}\right)=0, \tag{55}$$

where

$$Z=\frac{K_1(\alpha a)I_1'(\alpha)-I_1(\alpha a)K_1'(\alpha)}{I_1(\alpha)K_1(\alpha a)-I_1(\alpha a)K_1(\alpha)}. \tag{56}$$

At the next order, the equations used to derive the secular equation are (35), (45) with $B_1^{(1)}$ eliminated using (53), (47), and (54) with $D_2^{(1)}$ given by (50); the $B_3^{(1)}$ in these equations is given by (48). After tedious manipulation of these equations and using (55) to cancel some terms, the final result is simply

$$c_1=-(i/\mathbb{R}\alpha)(F/G), \tag{57}$$

where

$$F=\frac{(\kappa^2-\alpha^2)^2}{2p}\frac{Y[K_1'(\alpha)-K_1(\alpha)Z]}{K_1(\alpha a)}+\frac{H}{q}\left((\kappa^2-3\alpha^2)(\kappa^2-\alpha^2)\frac{Z}{2\alpha}-\frac{(\kappa^4-\alpha^4)}{2\alpha}\frac{I_1'(\alpha)}{I_1(\alpha)}-(\kappa^2-\alpha^2)+\frac{i\mathbb{R}}{\alpha(a^2-1)}(\kappa^2-3\alpha^2)\right),$$

$$G=-\left(1+\frac{\kappa^2-\alpha^2}{2\kappa}\frac{I_0(\kappa)}{I_1(\kappa)}\right)\frac{\kappa^2-\alpha^2}{2\alpha}Z+\frac{\kappa^2+\alpha^2}{2\alpha}\frac{I_1'(\alpha)}{I_1(\alpha)}\left(1+\frac{\kappa^2+\alpha^2}{2\kappa}\frac{I_0(\kappa)}{I_1(\kappa)}\right)-\frac{i\mathbb{R}}{\alpha(\alpha^2-1)}\frac{\kappa^2-\alpha^2}{2\kappa}\frac{I_0(\kappa)}{I_1(\kappa)}-\alpha^2+\frac{3(\kappa^2-\alpha^2)}{2\kappa}\frac{I_0(\kappa)}{I_1(\kappa)}-H,$$

$$H=\frac{1}{\kappa^2-\alpha^2}\left((\kappa^2-3\alpha^2)\kappa\frac{I_1'(\kappa)}{I_1(\kappa)}+(\kappa^2-\alpha^2)+(\kappa^2+\alpha^2)\alpha\frac{I_1'(\alpha)}{I_1(\alpha)}\right),$$

$$Y=\{\alpha a[I_1(\alpha)K_1(\alpha a)-I_1(\alpha a)K_1(\alpha)]\}^{-1}.$$

In the nonlinear equation (55) the eigenvalue c_0 is embedded in $\kappa^2=\alpha^2+i\mathbb{R}\alpha(1-c_0)$. Inspection of (55) and (57) shows that there are three parameters in the equations, the radius ratio a, the dimensionless wave number α, and the Reynolds number $\mathbb{R}$. The expansion (12) shows that the eigenvalue depends also on the viscosity ratio m. It is interesting to notice that up to this order the interfacial tension parameter $\hat{J}$ does not come into play.

One obvious solution to the Eq. (55) is $\kappa^2=\alpha^2$, but since $c_0\neq 1$ by the assumption in this section, this solution is rejected. Given a, α, and $\mathbb{R}$ the nonlinear equation (55) is solved numerically using IMSL subroutine ZANLYT and checked on the Macintosh II with software Mathematica. We found that there is only one root of κ^2 (or c_0) to this equation in the range of interest. After obtaining κ^2 we can easily calculate c_1 from (57), and eigenvalue c from

$$c=c_0+(\sqrt{m/\mathbb{R}\alpha})c_1. \tag{58}$$

The neutral curves are computed by fixing a and m, and searching the $(\alpha, \mathbb{R})$ plane for the line on which the growth rate of disturbances $\mathrm{Im}\{\alpha c\}=0$. Figure 2 present the neutral curves obtained in this case, for radius ratio $a=1.5$ and viscosity ratio $m=10^{-3}, 10^{-4}$, and 10^{-5}. The region to the right of these curves is stable, and to the left is unstable. We noticed that these neutral curves are almost parallel straight lines in the log–log plot with a shift for different viscosity ratios m, and they seem to fit the relation $\alpha_c=\mathrm{const}^*(m\mathbb{R})^{1/3}$. We also noticed that the neutral curves exist at relatively small wave number, or for long waves. Thus we carried out an asymptotic analysis of the secular equations (55) and (57) for small α, under the condition that $\sqrt{m/\mathbb{R}\alpha}$ is still a small parameter. In this case the eigenvalue c can be expressed as

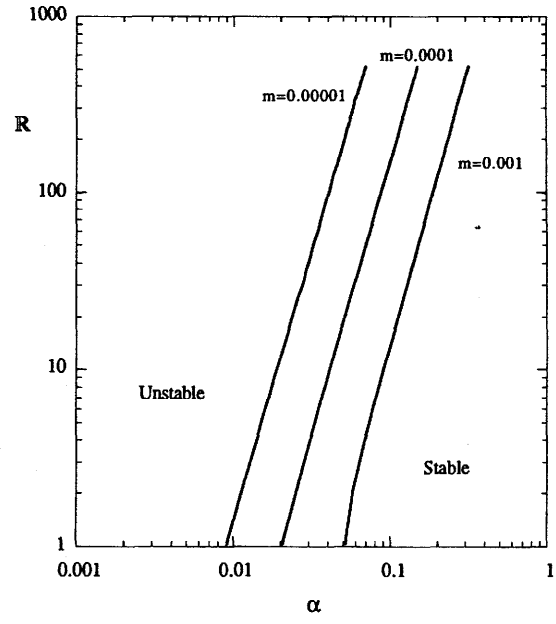

FIG. 2. Neutral curves for the case I in which the critical point is far away from the interface. The radius ratio is $a=1.5$ and the viscosity ratio $m=10^{-3}, 10^{-4}$, and 10^{-5}. The region to the right of the neutral curves is stable, and to the left is unstable. An asymptotic analysis for small α and small $\sqrt{m/\mathbb{R}\alpha}$ leads to a formula for the neutral curve $\alpha_c=0.6057[(m\mathbb{R})^{1/3}/(a^2-1)^{5/3}]$, or $\alpha_c=0.4176(m\mathbb{R})^{1/3}$ in the present case. This formula almost exactly fits the curves in the figure.

$$c=\frac{a^2-1}{a^2}-i\frac{3\alpha(a^2-1)}{\mathbf{R}a^2}$$
$$+\sqrt{\frac{m}{\mathbf{R}\alpha}}\frac{\sqrt{2}}{a^2(a^2-1)}\frac{1+i}{\sqrt{a^2-1}}. \tag{59}$$

The neutral curve is determined by $\mathrm{Im}\{c\}=0$, that is,

$$\alpha_c=\left(\frac{\sqrt{2}}{3}\right)^{2/3}\frac{(m\mathbf{R})^{1/3}}{(a^2-1)^{5/3}}=0.6057\frac{(m\mathbf{R})^{1/3}}{(a^2-1)^{5/3}}. \tag{60}$$

Equation (60) gives the lines presented in Fig. 2 almost exactly.

IV. CASE II: THE CRITICAL POINT IS CLOSE TO THE INTERFACE

In this section, we consider the case where the critical point is at a distance of order $\epsilon^{1/3}$ from the interface, as shown in Fig. 1(b). Unlike the previous case where the presence of the critical layer can be totally ignored, the critical layer in this case does play an important role.

We consider the expansion

$$c=1+\epsilon^{1/3}c_1+\cdots, \tag{61}$$

where $c_0=1$ and c_1 is the first-order correction.

An analysis similar to the one carried out in Sec. III is used to get the solutions in the core Ω_1, in the outer region of annulus Ω_2 and in the wall boundary layer Ω_{22}. Only one term of the expansion is computed. The results are listed below

$$u_1(r)=u_1^{(0)}(r)+O(\epsilon^{1/3}),\quad \text{in } \Omega_1,$$
$$u_1^{(0)}(r)=A_{11}I_1(\alpha r)+A_{12}rI_0(\alpha r); \tag{62}$$
$$u_2(r)=u_2^{(0)}(r)+O(\epsilon^{1/3}),\quad \text{in } \Omega_2,$$
$$u_2^{(0)}(r)=A_{21}I_1(\alpha r)+A_{22}K_1(\alpha r); \tag{63}$$
$$u_2(r)=\epsilon^{1/2}[u_{22}^{(0)}(\eta)+O(\epsilon^{1/3})],\quad \text{in } \Omega_{22},$$
$$u_{22}^{(0)}(\eta)=A_3^{(2)}[e^{p\eta}-p\eta-1]. \tag{64}$$

The matching of the wall boundary inner expansion (64) as $\eta=(a-r)/\epsilon^{1/2}\to\infty$ with the outer expansion (63) as $r\to a^-$ gives the equation

$$u_2^{(0)}(a)=0. \tag{65}$$

Inside the critical layer Ω_{21} near the interface, we introduce an inner variable

$$z=(r-1)/\epsilon^{1/3}, \tag{66}$$

and take a one term expansion for velocity

$$u_2(r)=u_{21}^{(0)}(z)+O(\epsilon^{1/3}). \tag{67}$$

Equation (4) at the leading order reduces to

$$D_z^4u_{21}^{(0)}+i[c_1+2z/(a^2-1)]D_z^2u_{21}^{(0)}=0. \tag{68}$$

The interfacial conditions (7)–(10), at $r=1$ (or $z=0$), become

$$u_{21}^{(0)}(0)=u_1^{(0)}(1), \tag{69}$$
$$c_1D_zu_{21}^{(0)}(0)=[2/(a^2-1)]u_1^{(0)}(1), \tag{70}$$
$$0=[D^2+D-1+\alpha^2]u_1^{(0)}(1), \tag{71}$$
$$\mathbf{R}\alpha D_z^3u_{21}^{(0)}(0)=[D^3+2D^2-(3\alpha^2+1)D+1-\alpha^2]u_1^{(0)}(1). \tag{72}$$

Consider an equation of the form

$$\frac{d^2\omega}{dz^2}+i\left(c_1+\frac{2z}{a^2-1}\right)\omega=0,$$

which is solvable with Airy functions

$$\mathrm{Ai}\left[-\left(\frac{2}{a^2-1}\right)^{1/3}\left(z+\frac{c_1}{2}(a^2-1)\right)e^{i\theta}\right],$$

where $\theta=\pi/6, 5\pi/6$, or $-\pi/2$. If we require that ω should be matched with some outer expansion as $z\to\infty$, the solution must tend to some finite value as $z\to\infty$. This limits the only possible solution to the value $\theta=5\pi/6$. Therefore the general solution of (68) has a form similar to the one for plane shear flow computed by Hooper and Boyd,[15,16]

$$u_{21}^{(0)}(z)=A_1^{(1)}+A_2^{(1)}z+A_3^{(1)}\chi(z), \tag{73}$$

where

$$\chi(z)=\int_\infty^z dz\int_\infty^z \mathrm{Ai}\left[-\left(\frac{2}{a^2-1}\right)^{1/3}\times\left(z+\frac{c_1}{2}(a^2-1)\right)e^{i5\pi/6}\right]dz. \tag{74}$$

The boundary conditions (69), (70), and (72) require that

$$A_1^{(1)}+A_3^{(1)}\chi(0)=u_1^{(0)}(1), \tag{75}$$
$$c_1[A_2^{(1)}+A_3^{(1)}\chi'(0)]=[2/(a^2-1)]u_1^{(0)}(1), \tag{76}$$
$$\mathbf{R}\alpha A_3^{(1)}\chi'''(0)=[D^3+2D^2-(3\alpha^2+1)D+1-\alpha^2]u_1^{(0)}(1). \tag{77}$$

The matching of this inner with the outer expansion (63) requires that

$$A_2^{(1)}=0, \tag{78}$$
$$A_1^{(1)}=u_2^{(0)}(1). \tag{79}$$

Equation (76) with $A_2^{(1)}=0$ and $A_3^{(1)}$ eliminated by (77) may be written as

$$\frac{2\mathbf{R}\alpha}{(a^2-1)c_1}\frac{\chi'''(0)}{\chi'(0)}[A_{11}I_1(\alpha)+A_{12}I_0(\alpha)]=-2\alpha^3[A_{11}I_1'(\alpha)+A_{12}I_1(\alpha)]. \tag{80}$$

This, together with Eq. (71) written as

$$A_{11}2\alpha^2I_1(\alpha)+A_{12}2\alpha[I_1(\alpha)+\alpha I_0(\alpha)]=0, \tag{81}$$

leads to the secular equation

$$\frac{1}{c_1}\frac{\chi'''(0)}{\chi'(0)}=\frac{\alpha(a^2-1)}{\mathbf{R}}\left(1+\alpha^2-\alpha^2\frac{I_0^2(\alpha)}{I_1^2(\alpha)}\right). \tag{82}$$

If we define a constant E independent of the unknown c_1

$$E=1-i\frac{\alpha(a^2-1)}{\mathbf{R}}\left(1+\alpha^2-\alpha^2\frac{I_0^2(\alpha)}{I_1^2(\alpha)}\right), \tag{83}$$

and use

$$x=\left(\frac{a^2-1}{2}\right)^{2/3}e^{-i\pi/6}\frac{c_1}{2} \tag{84}$$

as the new variable, we may use the properties of Airy function to write the secular equation (82) in a very simple form

$$\int_0^\infty (z+Ex)\mathrm{Ai}(x+z)dz = 0. \tag{85}$$

It is very interesting to notice that the unknown x in the equation depends only on E, a combination of three parameters: a, α, and $\mathbf{R}$. Therefore in the computation of neutral curve, we only need to find one neutral point at $E = E_c$ and $x = x_c$ which satisfies $\mathrm{Im}\{c_1\} = 0$. Then, using (83) we can extend this point to a whole curve on $(\alpha,\mathbf{R})$ plane valid for different values of a. The equation for this neutral curve is

$$\mathbf{R}_c = i\frac{(a^2-1)}{1-E_c}\alpha\left(1+\alpha^2-\alpha^2\frac{I_0^2(\alpha)}{I_1^2(\alpha)}\right).$$

We also note that although the total eigenvalue c depends on the viscosity ratio m, the neutral curve on which $\mathrm{Im}\{c\} = \mathrm{Im}\{c_1\} = 0$ is independent of m.

The Airy functions of complex argument was computed using an algorithm developed by Schulten, Anderson, and Gordon,[17] and the integration in (85) was transformed into interval [0,1] and integrated numerically using an adaptive scheme given by Robinson,[18] which was modified to handle the complex valued functions. The equation solver is subroutine ZANLYT on IMSL. And the results are again checked on Macintosh II with software Mathematica. In solving the nonlinear equation (85), we only choose the root c_1 that has a negative real part since the velocity of the disturbance equals to the basic flow velocity at the critical point which is always less than 1, and pick up the root with the largest imaginary part, or the most unstable mode with the largest growth rate.

We find numerically that $E_c = 1 + 0.425i$; thus the neutral curves are totally given by

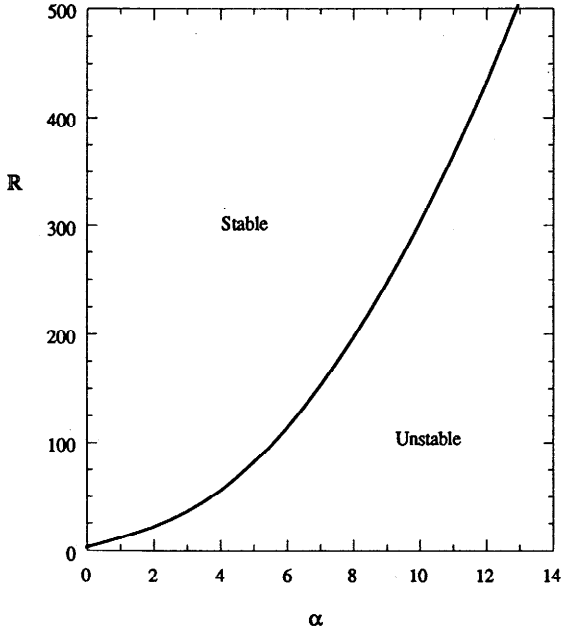

FIG. 3. Neutral curve for case II in which the critical point is close to the interface, when the radius ratio $a = 1.5$. The region to the right of the neutral curves is unstable, and to the left is stable. It is given by the equation $\mathbf{R}_c = 0.294(a^2-1)\alpha\{-1-\alpha^2+\alpha^2[I_0^2(\alpha)/I_1^2(\alpha)]\}$.

$$\mathbf{R}_c = 0.294(a^2-1)\alpha\{-1-\alpha^2+\alpha^2[I_0^2(\alpha)/I_1^2(\alpha)]\}. \tag{86}$$

In Fig. 3 we have plotted (86) for $a = 1.5$. The region to the right of the neutral curve is unstable, and the region to the left is stable. Thus the short waves (disturbances with large wave number α) are unstable, since the effect of interfacial tension is suppressed in the present study. If the effect of interfacial tension is to be included [we need to make some assumptions about the magnitude of the combination $(m^2\alpha\hat{J}/\mathbf{R})$ in the Eq. (10)], we expect to have another branch of neutral curve which stabilizes the short waves.

V. NUMERICAL COMPUTATION TAKING INTO ACCOUNT THE INTERFACIAL AND BOUNDARY LAYERS

The finite element code for linear stability computation of core-annular flow given in Hu and Joseph[9,10] is here modified to take into account the effects of the boundary layers near the pipe wall and near the interface between two liquids.

In the core region $0 \leqslant r \leqslant 1$, since the equation is regular, we use ten uniform elements in the code. While in the annulus $1 \leqslant r \leqslant a$, we first divide the annulus into eight equal intervals, then in the first interval (closest to the interface) and in the last interval (closest to the pipe wall), we generate elements whose size increases gradually with a magnification rate of 2. The size of the smallest element is kept less than

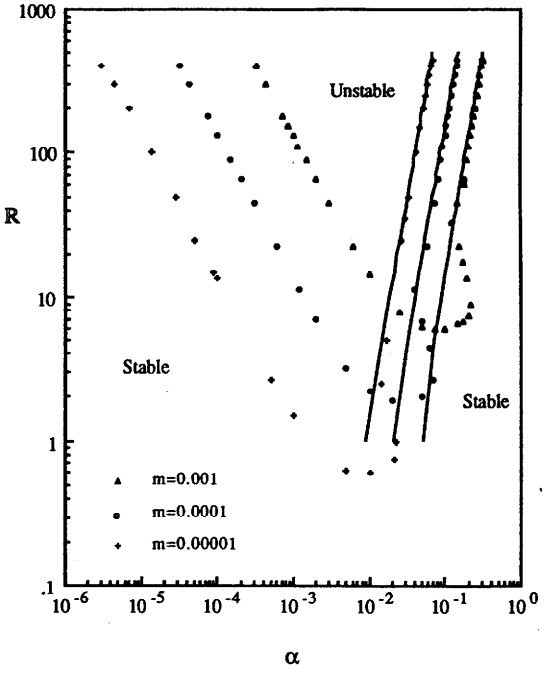

FIG. 4. Comparison of neutral curves corresponding to case I obtained by the matched asymptotic expansions (solid lines) with that obtained by the modified finite element code (dots). The radius ratio $a = 1.5$, surface tension parameter $\hat{J} = 0$ and viscosity ratio $m = 10^{-3}$, 10^{-4}, and 10^{-5}. The agreement is good at one end of the curves with large α. At the other end, the finite element code predicts another branch of neutral curve, while the method of matched asymptotic expansions method fails since $\sqrt{m/\mathbf{R}\alpha}$ is no longer a small parameter when α or $\mathbf{R}$ is extremely small.

$0.1\sqrt{m/\mathrm{R}\alpha}$, thus the number of the elements used in the program varies automatically according to the values of m, R, and α. This modified code is compatible with the old ones.

We made comparisons for the results obtained using this modified finite element code with those obtained by the matched asymptotic expansions method. Figure 4 shows the comparison of neutral curves at relatively small α, corresponding to case I in which the critical point is far away from the interface or the velocity of disturbances is not close to one. We see a very good agreement at one end of the curves. At the other end, the finite element code predicts another branch of neutral curve, while the matched asymptotic expansions method fails since $\sqrt{m/\mathrm{R}\alpha}$ is no longer a small parameter when α or R is extremely small. The long wave (small wave number α) analysis given by Preziosi, Chen, and Joseph[8] shows that the core-annular flow is always stable as $\alpha \to 0$ when interfacial tension is neglected, as confirmed by the finite element computation.

Figure 5 presents the comparison of neutral curves corresponding to the second case in which the critical point is near the interface or the velocity of disturbances is close to one. We observe an increasingly better agreement as $m \to 0$. Figure 6 combines the neutral curves in Figs. 4 and 5 giving an overall view of the neutral curves in the (α,R) plane.

Figure 7 demonstrates the changes of the neutral curves in the (α,R) plane as m increases when $\hat{J}$ is not zero ($a = 1.25$ and $\hat{J} = 1000$). The numerical solutions shown in Fig. 7(a) for $m = 0.001$ is similar to the neutral curves in Fig. 6, except that in Fig. 7(a) there exists an extra branch for $\alpha > 1$ at small R, which corresponds to the stabilizing

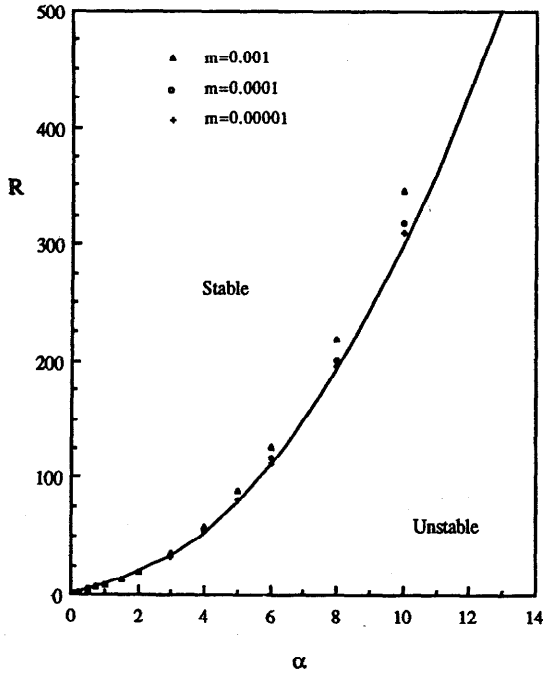

FIG. 5. Comparison of neutral curves corresponding to case II obtained by the matched asymptotic expansions [solid line given by Eq. (86)] with that obtained by the modified finite element code (dots). The radius ratio $a = 1.5$, surface tension parameter $\hat{J} = 0$ and viscosity ratio $m = 10^{-3}$, 10^{-4}, and 10^{-5}. The agreement is increasingly better as $m \to 0$.

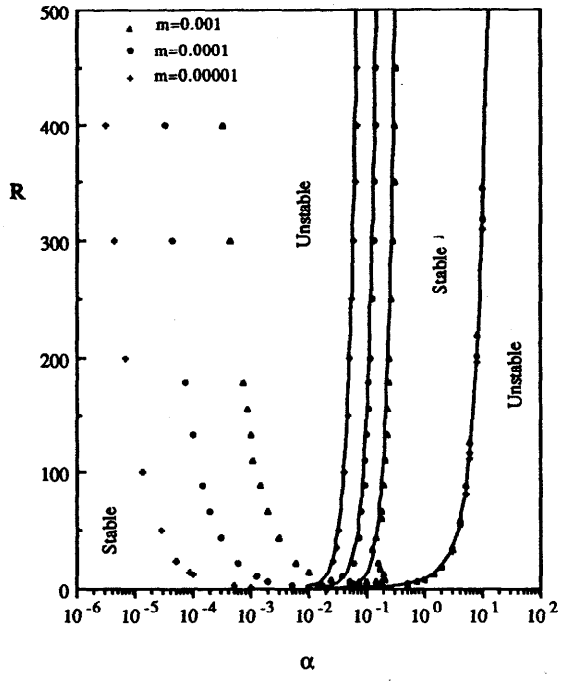

FIG. 6. Combination of Figs. 4 and 5. This gives an overall view of the neutral curves for both case I and case II.

effects of the interfacial tension for short waves. Since the effect of interfacial tension scales according to parameter $J^* = T\rho R_1/\mu_1^2 = \hat{J}m^2$, as m increases the influence of the interfacial tension increases quickly. In Fig. 7(b) ($m = 0.01$), the extra branch gets connected with the branch corresponding to the case II in asymptotic analysis and forms another U-shape branch at large α. At the left-hand side corner the small unstable bubble is caused by the capillary instability due to the interfacial tension. When $m = 0.1$, Fig. 7(c), the interfacial tension further stabilizes the short waves (pushs up the U-shape branch at large α) and destabilizes the long waves (blows the bubble at the left-hand side corner). If the $\hat{J}$ is large enough, the U branch at large α can be pushed out of sight. Then the U-shaped branch at small α and the bubble at the left-hand side corner are the familar upper and lower branches of neutral curves displayed in Preziosi, Chen, and Joseph[8] for finite but small m.

VI. GROWTH RATE AND WAVE VELOCITY

We know that $\mathrm{Im}\{\alpha c\}$ is the growth rate and $\mathrm{Re}\{c\}$ is the wave velocity for small disturbances. The two modes of instability corresponding to case I and case II have different growth rates. For $\mathrm{R} = 100$, $a = 1.5$, and $m = 0.001$, 0.0001, and 0.000 01, the growth rate for both modes are plotted in Fig. 8. The results are obtained using the method of matched asymptotic expansions. This figure shows that the growth rate for mode I, corresponding to case I, is small and positive at small α, it reaches a maximum at α about 0.1, which varies for different m, then decreases rapidly as α increases. The growth rate for mode II, corresponding to case II, has a peak at $\alpha = 12.1$ which is independent of m, and decays to zero at both ends of small and large α. Except at small α, the growth

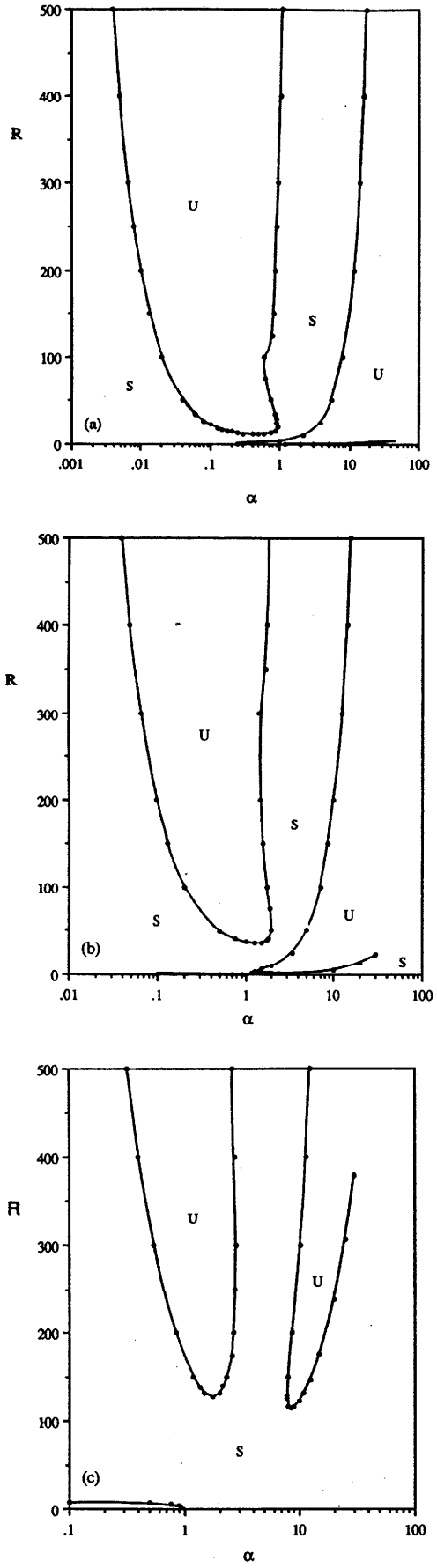

FIG. 7. Changes of the neutral curves as the viscosity ratio m increases. The radius ratio $a = 1.25$, surface tension parameter $\hat{J} = 1000$ and (a) $m = 0.001$; (b) $m = 0.01$; (c) $m = 0.1$. Here U and S indicate unstable and stable regions, respectively.

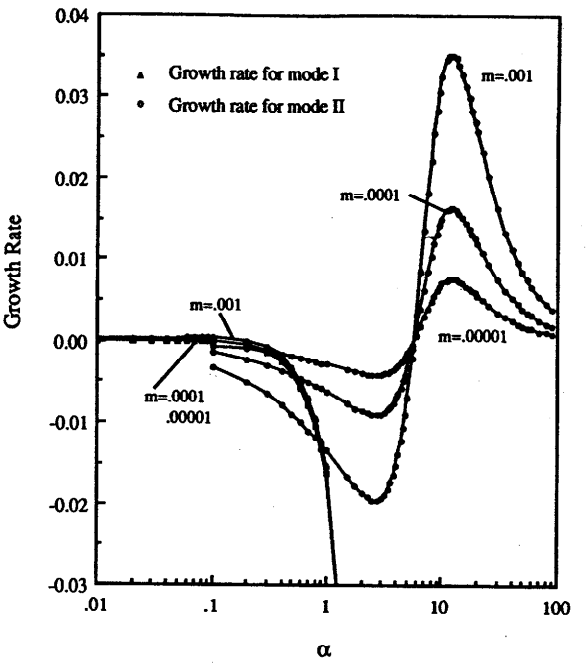

FIG. 8. Growth rates $\mathrm{Im}\{ac\}$ versus wave number α for two modes of instability when $\mathbf{R} = 100$, $a = 1.5$ and $m = 0.001$, 0.0001, 0.000 01. Δ is the growth rate for mode I corresponding to case I and $\bigcirc$ is the growth rate for mode II corresponding to case II. Except at small α where the growth rate of mode I is slightly positive and the growth rate of mode II is negative, the growth rate of mode II is much larger than that of mode I. The maximum growth rate occurs on the curve for mode II at $\alpha = 12.1$, and tends to zero (neutrally stable) as m tends to zero.

rate of mode II is much larger than that of mode I. Combining these two modes of instability the maximum growth rate for the whole range of α occurs on the curve for mode II at $\alpha = 12.1$. This maximum growth rate tends to zero (neutrally stable) as m tends to zero because the growth rate is proportion to $m^{1/3}$ as shown in expansion (61).

The energy analysis described in Hu and Joseph[9] using the finite element code shows that for the second mode of instability the B_2 term due to the difference of viscosity and interfacial friction is dominant in the energy balance. The comparison with experiments in Hu and Joseph[9] shows that this type of instability leads interfacial waves.

The wave velocities for the same parameter as in Fig. 8 at the maximum growth rates are 0.9961, 0.9982, 0.9991 for $m = 0.001$, 0.0001, and 0.000 01, respectively. The expansion (61) also shows that the interfacial wave tends to be stationary, the wave velocity is equal to the velocity of the core, as m tends to zero.

VII. CONCLUSIONS

(a) As the ratio of viscosities of water to oil m tends to zero ($\epsilon = m/\mathbf{R}\alpha$ as a small parameter), the equation that governs the linear stability of the core-annular flow is regular in the core of oil; and is singular in the annulus of water with boundary layers near the pipe wall and the interface, and with a critical layer whose position is not predetermined.

(b) According to the position of the critical point in annulus, there are two modes of instability. One is when the

critical point is far away from the interface, or the velocity of the disturbance is much less than one, corresponding to case I. The other is when the critical point is close to the interface within a distance of order $\epsilon^{1/3}$, corresponding to case II.

(c) In case I, the eigenvalue c is determined by (55) and (57). For small values of α and $\sqrt{m/R\alpha}$ the eigenvalue can be expressed explicitly by Eq. (59), and the neutral curve by Eq. (60). In case II, the eigenvalue c can be determined by solving the nonlinear equation (85), while the neutral curve is simply given by Eq. (86) explicitly.

(d) The finite element code with more elements introduced by an adaptive method in the boundary layers near the pipe wall and the interface works well for the cases of small viscosity ratio, and agrees well with the results obtained by the matched asymptotic expansions method where the two coincide. The finite element method has no limitation and gives good results globally in parameter space.

(e) The instability of the core-annular flow, when the viscosity ratio m is small, leads to an interfacial wave with wave velocity slightly less than the velocity of the interface. As m tends to zero, the interfacial wave tends to a standing wave convected with the velocity of the flow at the interface and the maximum growth rate tends to zero; we get a neutrally stable standing wave in a coordinate system moving with velocity of the interface.

ACKNOWLEDGMENTS

This work was supported by the Department of Energy, the National Science Foundation, and the Army Research Office, Mathematics. Computer results were obtained under a grant from the Minnesota Supercomputer Institute.

[1] D. D. Joseph, K. Nguyen, and G. Beavers, J. Fluid Mech. **141**, 319 (1984).
[2] T. W. F. Russell and M. E. Charles, Can. J. Chem. Eng. **39**, 18 (1959).
[3] T. W. F. Russell, G. W. Hodgson, and G. W. Govier, Can. J. Chem. Eng. **37**, 9 (1959).
[4] M. E. Charles, G. W. Govier, and G. W. Hodgson, Can. J. Chem. Eng. **39**, 17 (1961).
[5] M. E. Charles and L. U. Lilleleht, Can. J. Chem. Eng. **44**, 47 (1966).
[6] R. Bai, K. Chen, and D. D. Joseph, submitted to J. Fluid Mech.
[7] D. D. Joseph, Y. Renardy, and M. Renardy, J. Fluid Mech. **141**, 309 (1984).
[8] L. Preziosi, K. Chen, and D. D. Joseph, J. Fluid Mech. **201**, 323 (1989).
[9] H. H. Hu and D. D. Joseph, J. Fluid Mech. **205**, 359 (1989).
[10] H. H. Hu and D. D. Joseph, Phys. Fluids A **1**, 1659 (1989).
[11] P. G. Drazin and W. H. Reid, *Hydrodynamic Stability* (Cambridge U.P., Cambridge, 1979).
[12] D. T. Papageogiou, C. Maldarelli, and D. S. Rumschitzki, Phys. Fluids A **2**, 340 (1990).
[13] J. Kevorkian and J. D. Cole, *Perturbation Methods in Applied Mathematics* (Springer, Berlin, 1980).
[14] M. Van Dyke, *Perturbation Methods in Fluid Mechanics* (Parabolic, Stanford, CA, 1975).
[15] A. P. Hooper and W. G. C. Boyd, J. Fluid Mech. **128**, 507 (1983).
[16] A. P. Hooper and W. G. C. Boyd, J. Fluid Mech. **179**, 201 (1987).
[17] Z. Schulten, D. G. M. Anderson, and R. G. Gordon, J. Comput. Phys. **31**, 60 (1979).
[18] I. Robinson, Aust. Comput. J. **8**, 106 (1976).